Continuous Fixed Bed Ligand Exchange: The Shrinking-Core Model

Wayne B. Bolden
Ted White
Frank R. Groves, Jr.
Chemical Engineering Department
Louisiana State University
Baton Rouge, LA 70803

Ligand exchange is a process in which small amounts of a solute, the ligand, may be removed from solution by complexing with an immobilized metal ion. For example, ammonia may be removed from water by complexing with Cu(II) held on a cation exchange resin. The process is carried out in a continuous fixed bed of resin particles much like an ion exchange column. Ligand exchange has interesting potential as a pollution control process and as a separation method for biochemical products produced in dilute solution.

In ligand exchange, complexing is rapid and rate is mass-transfer controlled. Moreover, the reaction equilibrium strongly favors the complex yielding an equilibrium curve that is close to a step function. This is the situation for ammonia or amine complexing with copper, provided the solution concentration exceeds ~0.1 M. Under these conditions an amine molecule diffusing into a resin pellet will be immediately complexed when it encounters a copper ion and will thereafter remain attached. A fully complexed region develops and advances inward. A core of uncomplexed Cu(II) shrinks toward the center of the pellet. Thus the process conforms to the shrinking core model, familiar from gas-solid reaction studies.

This note describes a mathematical model for fixed bed ligand exchange using the shrinking core model to describe the exchange rate at any point in the bed.

Previous Work

Bolden (1986) applied the pore diffusion model in a numerical solution for batch and fixed-bed ligand exchange. The pore diffusion model gives a rigorous description of mass-transfer controlled sorption but requires solution of the partial differential equation for diffusion in the resin pellet. Although the model successfully represented fixed-bed data for aliphatic amines complexing with Cu(II), the numerical solution consumed considerable computer time.

Correspondence concerning this paper should be addressed to F. Groves, Jr.

The shrinking-core model with the psuedosteady-state approximation results in an ordinary differential equation for the pore diffusion process. Helfferich (1965) recognized that shrinking-core behavior could occur in ion exchange. Others (Dana and Wheelock, 1974; Hall and Sontheimer, 1977; Yoshida et al., 1987) verified shrinking-core behavior experimentally and gave numerical solutions for batch sorption. Bolden and Groves (1988) used this approach to model batch sorption of ammonia on a Cu(II) loaded resin. Agreement with experiment was good and the solution required much less computer time than the pore diffusion model.

Fixed Bed Ligand Exchange Using Shrinking Core Model

Consider a fixed bed, length L, of spherical resin beads loaded with Cu(II). At zero time a solution containing concentration C_o of amine is admitted. Our objective is to predict amine concentration in the solution, $C(x,t)$, and in the resin, $q_a(x,t)$, as functions of position in the bed and time.

In the shrinking-core treatment the sorption rate is governed by pore diffusion in the complexed outer shell. The appropriate mathematical description is the unsteady-state diffusion equation with a moving boundary for the diffusion region. This equation is greatly simplified if the psuedosteady-state approximation, $\partial C_p/\partial t = 0$, is valid for the diffusion process. Bischoff (1963) has shown that this approximation holds, provided that the adsorbed phase concentration is large compared to the solution concentration: $C_o/q_m\rho_p) \ll 1.0$. The diffusion equation then becomes an ordinary differential equation. In dimensionless form, the result (Smith, 1970) is:

$$\frac{\partial X}{\partial \Theta} = \frac{3C^*}{\left[\left(\frac{1}{(1-X)^{1/3}} - 1\right) + B_1\right]} \tag{1}$$

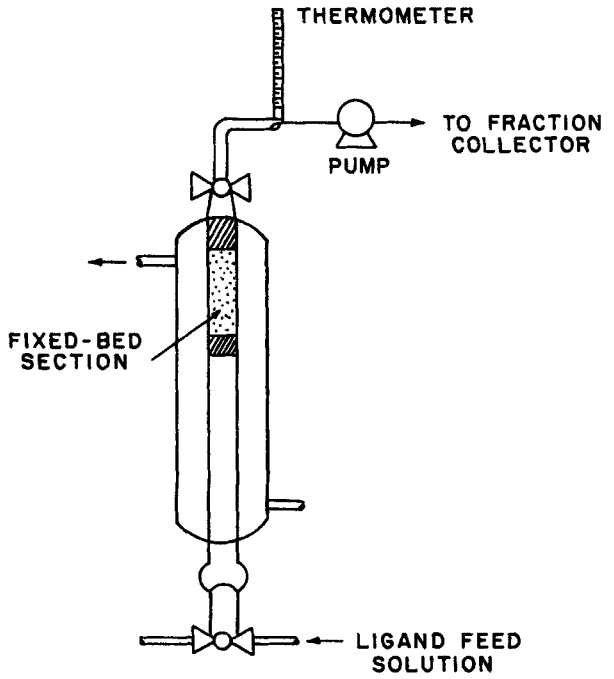

Figure 1. Experimental equipment for continuous ligand exchange.

The material balance on the ligand exchange bed is:

$$\frac{\partial C^*}{\partial x^*} = \frac{-3A_1 C^*}{\left[\left(\frac{1}{(1-X)^{1/3}} - 1\right) + B_1\right]} \tag{2}$$

Boundary conditions are:

$$C^* = 1.0 \quad \text{at} \quad x^* = 0 \quad \text{for all} \quad \theta > 0 \tag{3}$$

$$X = 0.0 \quad \text{at} \quad \theta = 0 \quad \text{for all} \quad x^* \tag{4}$$

Numerical Solution

Equations 1 and 2 are simultaneous hyperbolic partial differential equations. The independent variables, x^* and θ, are the characteristic coordinates. Since each equation contains a single independent variable, methods used for ordinary differential equations can be adapted for their integration. A simple predictor-corrector method was applied alternately to Eq. 1 and 2 to extend the region of known C^* and X from the boundaries, $x^* = 0$ and $\theta = 0$, to the interior of the plane.

Experimental Results

Breakthrough curves were obtained for butylamine and ammonia on laboratory columns containing Amberlite IRC-50 carboxylic acid type cation exchange resin, 20/50 mesh, loaded with Cu(II). Figure 1 shows the experimental equipment. Samples of column effluent were analyzed for amine by titration with dilute hydrochloric acid. Atomic absorption analysis of the effluent revealed no loss of copper. Table 1 summarizes experimental conditions. Figures 2, 3, and 4, show the breakthrough curves for ammonia and butyl amine.

Shrinking-Core Fit

The lines on the figures are predicted curves based on the shrinking-core model. Table 1 includes values of the external mass-transfer coefficient and effective diffusivity used. The mass transfer coefficient was obtained from an empirical correlation (Sherwood et al., 1975). The effective diffusivity was used as an adjustable parameter. The dotted lines on Figure 3 show the sensitivity of the results to changes in effective diffusivity. The resin concentration at saturation, q_m, was fitted to the material balance on the column.

Also shown in the table is $(C_o/q_m\rho_p)$, the parameter which determines whether the psuedosteady-state approximation is valid. For the dilute butylamine solutions, the parameter is small enough that the approximation is clearly satisfied. For the ammonia solutions the psuedosteady-state assumption is borderline. Nevertheless, the simplified shrinking core model gives a

Table 1. Experimental Conditions and Parameters for Breakthrough Curves

	Experiment			
	TW2	TW3	BAL-1	BAL-2
Ligand	NH	NH_3	Butylamine	
Column ID, cm	1.08	1.08	0.84	0.84
Feed rate, cm^3/s	0.0184	0.024	0.019	0.021
Bed length, cm	13.21	13.80	10.32	9.97
Resin mass in bed, g	3.92	4.09	2.00	1.93
Resin pellet dia., cm	0.03	0.03	0.03	0.03
Bed void fraction	0.36	0.36	0.36	0.36
Resin pellet density, g/cm^3	0.55	0.55	0.55	0.55
Resin pellet void fraction	0.38	0.38	0.38	0.38
Feed conc. mg/cm^3	3.720	1.399	0.223	0.195
Max. resin-phase conc., mg/g	170.8	123.1	240	212
Max. moles ligand/atom Cu	3.5	2.5	1.1	1.1
	0.04	0.021	0.0017	0.0017
Mass-transfer coeff., cm/s	0.0029	0.0039	0.0026	0.0027
Effective diffus., cm^2/s	4.0×10^{-7}	4.0×10^{-7}	3.0×10^{-7}	5.0×10^{-7}
Molecular diffus.,* cm^2/s	1.64×10^{-5}	1.64×10^{-5}	8.3×10^{-6}	8.3×10^{-6}
Tortuosity factor	16	16	10	6.3

*Sherwood et al. (1975)

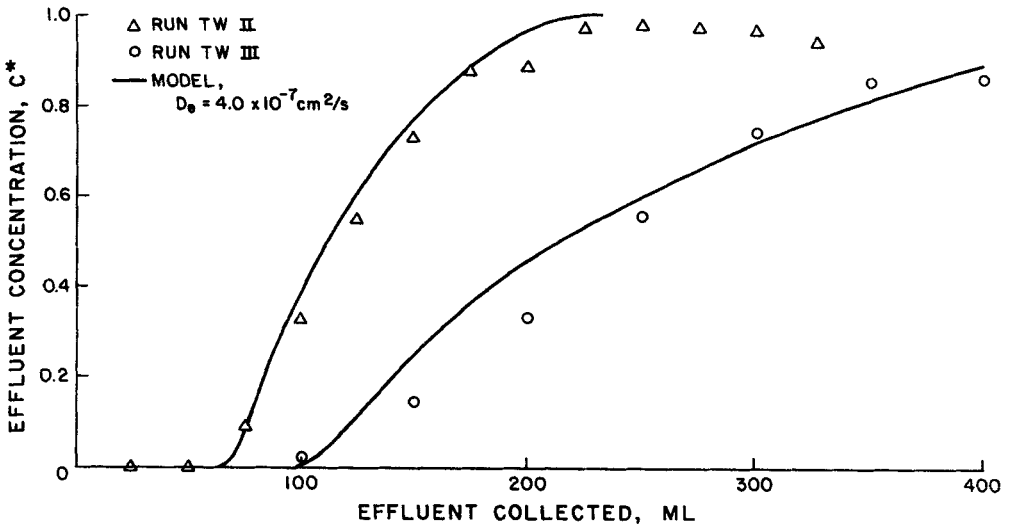

Figure 2. Breakthrough curve for ammonia.

good fit. In fact, for the ammonia data, the same effective diffusivity fits runs at rather widely varying conditions.

The effective diffusivity is related to molecular diffusivity through the void fraction and tortuosity factor of the solid.

$$D_e = \frac{\epsilon_p D}{f} \tag{5}$$

The calculated tortuosity factor is shown in Table I.

Discussion

Two parameters, q_m and D_e, were used in fitting the shrinking-core model to the data. The resin loading, q_m, in the complexed region was determined from the material balance on the column. This maximum resin loading depended on the concentration of ligand in the feed, corresponding to 1.0—3.5 molecules of ligand per atom of copper in the fully complexed region. The values of q_m from the column material balance were consistent with data from separate batch equilibrium experiments. Thus in using the model for design purposes, it should be possible to obtain q_m independently from such batch data.

The fitted values of D_e were smaller than anticipated. Calculated tortuosity factors for ammonia exceeded the range of 3 to 10 reported by Satterfield (1970) for porous catalyst pellets. Moreover, D_e for ammonia was an order of magnitude lower than obtained by Bolden and Groves (1988) by applying the shrinking-core model to batch data for the same resin.

This discrepancy for ammonia can be explained by the fact that the feed concentration for the column experiments was greater by a factor of 10, than for the batch data. In the batch experiments the fully complexed shell penetrated only slightly into the solid pellets (final fractional conversion, $X < 0.15$). Thus the batch data may not reflect the true tortuosity. Moreover, the copper ions, complexed with several ammonia molecules, may be bulky enough to partially block the pores. Finally at the low feed concentration of the batch experiments the equilibrium curve deviates from the step shape that produces shrinking-core behavior.

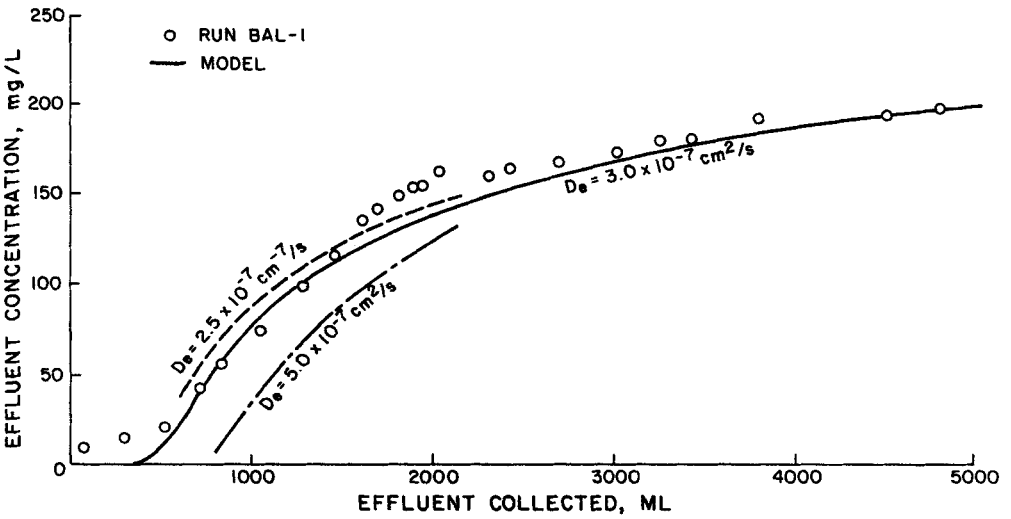

Figure 3. Breakthrough curve for butylamine-sensitivity to D_e.

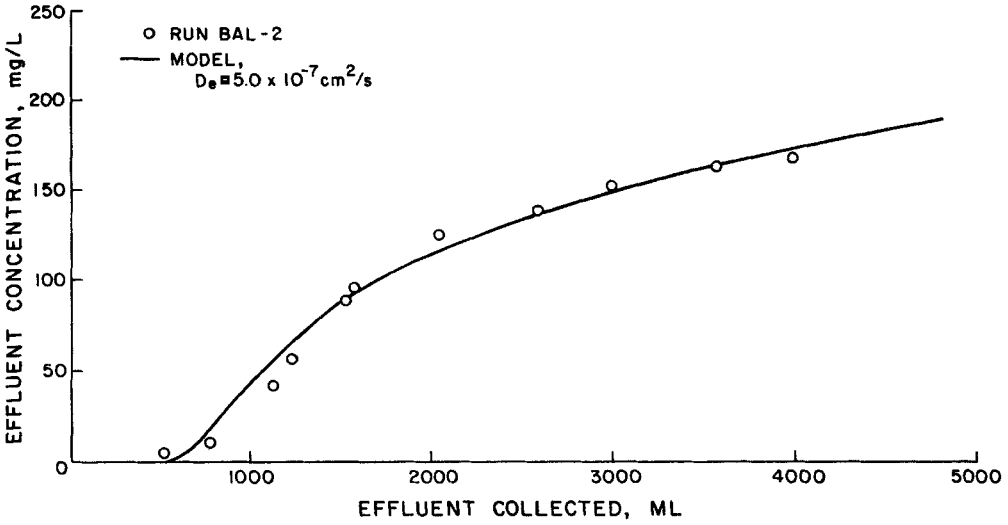

Figure 4. Breakthrough curve for butylamine.

For the butylamine, the tortuosity factor is within the anticipated range.

The shrinking-core model for ligand exchange has distinct advantages. When used with the psuedosteady-state approximation it leads to an ordinary differential equation for the exchange rate. This yields savings in computer time and reduction in program complexity compared to the rigorous pore diffusion model. The latter requires the solution of a partial differential equation for diffusion in the resin pellet—a much more complex computation.

Notation

A_1 = parameter, $(1 - \epsilon_b)LD_e/\epsilon_b vR^2$
B_1 = parameter, $D_e/(Rk_f)$, a Biot number
C = adsorber bulk liquid concentration, mg/cm^3
C_p = liquid phase concentration in resin pores, mg/cm^3
C_o = initial adsorber liquid concentration, mg/cm^3
C^* = dimensionless liquid concentration, C/C_o
D = molecular diffusivity, cm^2/s
D_e = resin pellet effective diffusivity, cm^2/s
f = tortuosity factor
k_f = boundary layer mass-transfer coefficient, cm/s
L = length of bed, cm
q_a = average resin phase concentration, mg/g
q_m = resin phase concentration in fully complexed zone, mg/g
R = bead radius, cm
t = time, s
v = interstitial velocity of fluid in bed, cm/s
x = distance from bed inlet, cm
x^* = distance, x/L
X = fractional conversion of resin beads

Greek letters

ϵ_b = bed void fraction
ϵ_p = pellet void fraction
ρ_b = bed bulk density, g/cm^3
ρ_p = pellet density, g/cm^3
$\theta = (1 - \epsilon_b)D_e C_o/\rho_b q_m R^2/t'$

Literature Cited

Bolden, W. B., "Amine Removal from Aqueous Process Streams by Ligand Exchange," Ph.D. Dissertation, Louisiana State University (1986).

Bolden, W. B., and F. R. Groves, "Batch Sorption by Ligand Exchange: Determination of Intraparticle Diffusivity," *Chem. Eng. Commun.*, **64**, 125 (1988).

Dana, P. R., and T. D. Wheelock, "Kinetics of a Moving Boundary Ion Exchange Process," *Ind. Eng. Chem. Fund.*, **13**, 20 (1974).

Helfferich, F., "Ion Exchange Kinetics: V. Ion Exchange Accompanied by Reactions," *J. Phys. Chem.*, **69**, 1178 (1965).

Höll, W., and H. Sontheimer, "Ion Exchange Kinetics of the Protonation of Weak Acid Ion Exchange Resins," *Chem. Eng. Sci.*, **32**, 755 (1977).

Satterfield, C. N., *Mass Transfer in Heterogeneous Catalysis*, M.I.T. Press, Cambridge, 35 (1970).

Sherwood, T. K., R. L. Pigford, and C. R. Wilke, *Mass Transfer*, McGraw-Hill, New York, 25 (1975).

Smith, J. M., *Chemical Engineering Kinetics*, 2nd ed., McGraw-Hill, New York, 576 (1970).

Yoshida, H., T. Kataoka, and S. Fukikawa, "Kinetics in a Chelate Ion Exchange: I. Theoretical Analysis; II. Experimental," *Chem. Eng. Sci.*, **41**, 2517 (1986).

Manuscript received July 11, 1988, and revision received Dec. 2, 1988.